

VORTEX BLOB METHOD AS VISUALIZATION TOOL FOR MULTI-ELEMENT AIRFOIL FLOWS OPTIMIZATION

Carmine GOLIA, Bernardo BUONOMO
Department of Aerospace & Mechanical Engineering
Second University of Naples, Italy

Abstract

Main scope of this work is to analyze the usefulness of Vortex Blob Method (VBM) in the visualization of flows around high lift systems, composed by multiple elements airfoils, in order to verify the optimality of settings and geometries.

After a brief presentation of VBM and its application in the Lagrangian approach to the solution of the unsteady Helmholtz formulation of the complete Navier-Stokes equations, we consider as reference airfoil the GA(W)-2 in plain configuration: as 2 elements high lift system (main combined with a slat), and as 3 elements high lift system (main combined with both a slat and a flap).

For each case, flow paths (blob vortex trajectories), velocity plots and load pressure distributions are presented as still frames of a computational movies.

The behaviour of the results of configurations and settings is physically reasonable for lift, not for drag and moment.

So, we can consider positively the use of Vortex Blob Method as a tool for flow visualization in the framework of a preliminary optimization process of complicated flow interactions among multi-element airfoils configurations at Reynolds number of engineering interest.

1 General Introduction

High-Lift Systems (HLS) have a major influence on the sizing, economics, and safety of most transport airplane configurations. The combination of complexity in flow physics, geometry, system support and actuation has

historically led to a lengthy and experimental intensive development process [1]. However, during the recent past, engineering design has changed significantly as a result of the rapid development in computational hardware and software.

The design of multi-element high-lift systems for aircraft has become increasingly important. Where early attention was mostly focused on maximum lift requirements to satisfy the cruise high wing-loading needs of jet transport aircraft while retaining acceptable takeoff and landing distances, more recently the attention has turned to reducing the complexity and weight of the high lift systems for given maximum lift levels.

Multi-element high lift systems have a significant impact on the cost of a typical jet transport because: (i) they are time consuming to design and test, (ii) their flows, geometry, and actuation and support systems are complex, (iii) they are heavy, (iv) have a high part count, and (v) are maintenance intensive.

According to Rudolph [2], an aircraft's high-lift system accounts for somewhere between 6% and 11% (potentially higher for more complex configurations) of the production cost of a typical jet transport.

The importance on aircraft performances of high lift systems is presented by Meredith [3] for a generic large twin jet engine transport:

- An increase in maximum lift coefficient of 1.0% translates into an increase in payload of 22 passengers or 4400 lb for a fixed approach speed on landing;
- An improvement in lift-to-drag ratio of 1.0% during takeoff translates into an increase in payload of 14 passengers or 2800 lb for a given range.

This example demonstrates that relatively small changes in the aerodynamic performance of the high lift system can produce large payoffs in airplane weight and performance.

This sensitivity of airplane weight and performance to small changes in high-lift aerodynamics in combination with the large impact of high lift systems on airplane cost explains why high-lift systems and their aerodynamic characteristics remain in the forefront of aerospace research. Fig. 1 illustrates the typical effect of a multi-element high lift system on lift. A leading-edge device, such as a slat, increases the stall angle of attack, whereas a trailing edge device, such as a single-slotted Fowler flap, produces an upward shift in the lift curve.

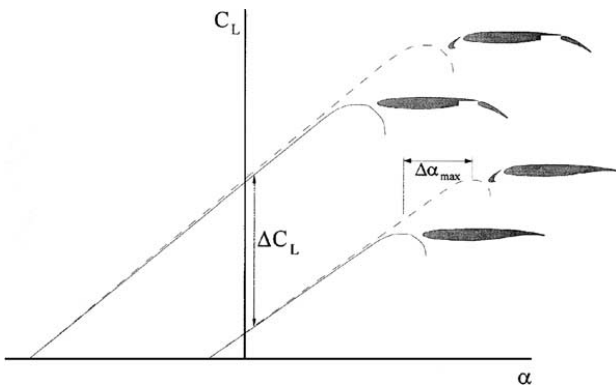


Fig. 1: Typical high lift system and its effect on airplane lift.

Although high lift systems are complex and costly, they are necessary to allow airplanes to take off and land on runways of acceptable length without penalizing the cruise efficiency significantly, as discussed in the following section.

2 Flow physics of multi-element high lift system

The problem of high lift aerodynamics has been studied since the early years of aviation but only in the 1970s significant progress was made in formulating a theoretical basis for high lift aerodynamics as a result of the insight into the underlying aerodynamic principles provided by A.M.O. Smith [4], who laid out the five predominant favorable effects of gaps (or slots) in multi-element airfoils flow.

The circulation of a forward element induces flow on a trailing element counter to the natural acceleration around the leading edge. This so called **slat effect** reduces the leading-edge suction peak on the trailing element, thus reducing pressure recovery demands and delaying separation.

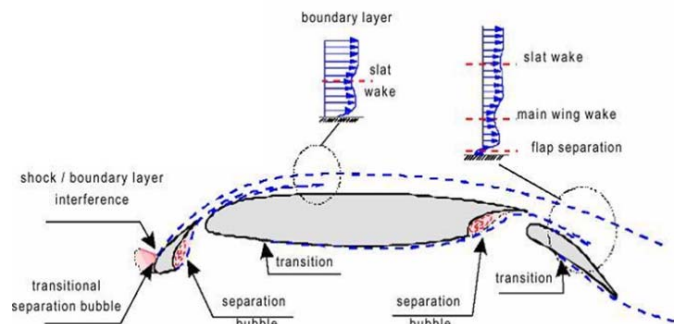


Fig. 2: Flow physics of multi-element high lift airfoil

The trailing element, however, induces a **circulation effect** on the forward element which tends to increase the loading on the forward element, increasing the lift, but also increasing pressure recovery demands. Yet, the high velocity flow on the upper surface of the trailing element allows the flow to leave the forward element at a higher speed. This **dumping effect** reduces the pressure recovery of the forward element and favours **off-surface pressure recovery**, which is more efficient than the recovery in contact with a wall. Finally, each element has a **fresh boundary layer** which originates on that element. A thin turbulent boundary layer can withstand stronger pressure gradients than a thick one and is less likely to separate.

Effectively, the overall pressure recovery of the multi element system is divided among all the elements, and the boundary layer does not continuously grow along the chord as it would for a single element system. The primary viscous effect of the gaps is the existence of individual wakes from each element of the system. These wakes are thought to provide a damping effect on the pressure peak of trailing elements, reducing the tendency of the flow to separate. Yet, the wakes often tend to merge with the boundary layer of the trailing element. The resulting confluent boundary layer is much

thicker than an ordinary boundary layer, so the likelihood of separation increases.

Clearly, optimizing the gap size requires a balance between the inviscid and viscous effects which favour smaller and larger gaps, respectively.

The aerodynamic problem of HLS lays in the capacity to describe and to recognize the physics of:

- Separation bubbles,
- Re-attachment,
- Re-laminarization,
- Confluence of boundary layer with wakes,
- Unsteady separated boundary layer.

All these problems are strongly dependent on the values of the flight Reynolds number.

The correct scaling and simulation of boundary-layer flows over wings in the high lift configuration is strongly dependent on the type and location of transition. The attachment-line boundary layer can be laminar, transitional, or turbulent, depending on the pressure distribution, the leading-edge sweep angle, the Reynolds number, and surface roughness and flow contamination. If attachment-line transition occurs, the resulting changes in the development of boundary layer flows can significantly influence the downstream turbulent flow field (i.e., confluent boundary layers and onset of separation).

Re-laminarization of the flow downstream of a turbulent attachment line can occur if the streamwise flow acceleration is sufficiently strong. If the flow ahead of a steep adverse pressure gradient along the upper surface of the elements is laminar, an additional Reynolds number effect can occur due to the presence of a laminar-separation bubble and its effect on subsequent turbulent-flow behaviour. The issues of leading-edge transition and re-laminarization are important in the extrapolation of sub-scale, three-dimensional, wind-tunnel results to full-scale flight conditions.

In aerodynamic design, computational methods [5] are slowly superseding empirical methods and design engineers are spending more and more time applying computational tools instead of conducting physical experiments to design and analyze aircraft including their high lift systems.

Typically, the wind-tunnel testing is the last issue of HLS design chain. The experimental data are used to extrapolate maximum lift to flight conditions obtained at Reynolds numbers where wing stall is dominated by conventional scale effects. Conventional scale effects refer to the increase of maximum lift with Reynolds number due to thinning of the turbulent boundary layer in the wing trailing edge region and subsequent aft shift of the trailing-edge flow separation point. At higher flight Reynolds numbers, attachment-line transition can occur, causing turbulent flow to start from the attachment line. By shifting the starting point of the turbulent boundary layer forward, the trailing-edge separation location can also shift forward due to the increased growth of the turbulent boundary layer. Because of the increased extent of trailing-edge separation, a significant reduction in maximum lift may occur. However, because steep favorable pressure gradients associated with high lift flows, relaminarization is also possible for some sections of the wing and would alleviate some of the lift loss due to attachment-line transition. For multi-element sections, there is also the effect of increased effective flap gap due to the thinning of the boundary layers at higher Reynolds numbers.

2 Vortex Blob Method (VBM) Fundamentals

We focus on the Lagrangian approach to continuum problems made discrete using a particle (blob) approach.

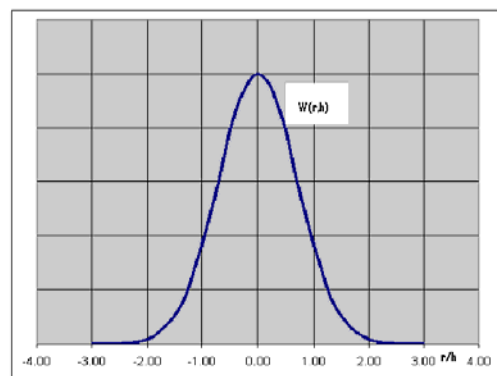


Fig. 3: Blob as a discrete Dirac representation

In this approach the Dirac representation:

$$f(\underline{x}) \cong \int \delta(\underline{x} - \underline{x}') f(\underline{x}') d\underline{x}' \quad (1)$$

is made discrete as a convolution integral:

$$f(\underline{x}) \cong \int W(\underline{x} - \underline{x}', h) f(\underline{x}') d\underline{x}' \quad (2)$$

where:

- $W(\underline{r}, h)$ is a convolution Kernel function satisfying given moment properties;
- h is the reference grid spacing.

In the limit $h \rightarrow 0$ the two representation shall coincide.

Blobs are then Dirac masses that directly translate and transport extensive properties as momentum, energy, charges, etc.

VBM uses individual discrete particles (blobs) that, as computational elements, transport momentum and energy. Blob particles move with velocity induced by vorticity field combined with basic potential flow, and exchange momentum and energy with neighborhood according to diffusive process. Local vorticity is created by no-slipping boundaries and, if the case, by thermal buoyancy.

The discrete representation considers the value of the field property “ f ” of the **p-th** blob computed as:

$$f(\underline{x}_p) \cong \sum_q W\left(\frac{\underline{x}_p - \underline{x}_q}{h}, h\right) \frac{f(\underline{x}_q)}{h^D} \Delta Vol_q \quad (3)$$

where:

- ΔVol_q is the volume of the q-blob;
- D is the dimension of the physical space.

After “*mollification*” (**allows overlap**) it follows:

$$f(\underline{x}_p) \cong \sum_q W\left(\frac{\underline{x}_p - \underline{x}_q}{\sigma}, h\right) \frac{f(\underline{x}_q)}{h^D} \Delta Vol_q \quad (4)$$

where:

- $\sigma = h \gamma$ is the blob radius;
- γ is an overlap parameter ($1 \div 1.5$).

It can be shown that blob methods represent exact weak solution for any admissible test function (local space averaged equation), i.e blob particle method achieve some (implicit) subgrid scale model.

Blob methods then differ from classical grid techniques since they do not involve projection of the equation in a finite dimensional space.

2.1 Governing equations

We focus on the application of the Lagrangian approach to the unsteady Helmholtz formulation of the complete Navier-Stokes equations, see [6] for an recent literature survey.

The analysis is performed, by using a splitting technique introduced by Chorin [7] that, by explicitly separating convective and diffusive steps, recasts the equations in a hyperbolic problem for the trajectories and a parabolic problem for the diffusive phenomena along the particles paths (*characteristics lines*).

Convective step

$$\frac{d\underline{r}_p}{dt} = \underline{V}_p(t) \quad (5)$$

Diffusive step:

$$\frac{d\underline{\omega}_p(t)}{dt} = \underbrace{\underline{\nabla} \cdot (\underline{\omega}_p(t) \underline{V}_p(t))}_{=0 \text{ in 2D}} + \nu \nabla^2 \underline{\omega}_p(t) \quad (6)$$

In regularized vortex blob method, the discretization of the equations is made by considering N-blobs problems where vorticity, for a general particle located in (\underline{r}, t) , is represented as convolution integrals on a compact domain around the blob particle:

$$\begin{aligned} \omega_q(t) &= \int_{\Omega} \omega_p(t) W(\underline{r}_q - \underline{r}_p, h) d\Omega_p \cong \\ &\cong \sum_{p \in \text{Cluster of } q} W(\underline{r}_q - \underline{r}_p, h) \Gamma_p(t) \end{aligned} \quad (7)$$

where $\Gamma_p(t)$ is the “*vortex blob intensity*” (i.e. the elementary circulation of the velocity) of the p-particle at time t .

The velocity field needed in (5) is sum of the potential field and of the one induced by the

vortex blobs (automatically divergence free). This last term can be represented as a convolution integral of the vorticity field (extension of the Biot-Savart law in free space, via Green's theory):

$$\underline{V}^{2D}(\underline{r}, t) = -\frac{1}{2\pi} \iint \left[\frac{(\underline{r} - \underline{r}') \wedge \underline{k} \omega(\underline{r}', t)}{|\underline{r} - \underline{r}'|^2} \right] d\underline{r}' \quad (8)$$

2.2 Core Spreading Method (CSM)

In this paper the diffusive Laplacian operator is made discrete according to the Core Spreading Techniques (CSM) introduced by Kuwahara & Takami [8] and Leonard [9].

The main idea is that if one consider, as kernel, a Gaussian distribution function such as:

$$W(\underline{x}, t) = \frac{\exp[-x^2/(4\nu t)]}{4\pi \nu t} \quad (9)$$

the blob core (σ) expands in time according to:

$$\frac{d\sigma^2}{dt} = k \nu \quad ; \quad k = (2.242)^2 \quad (10)$$

and satisfies identically the viscous part of the classical vorticity transport equation.

Greengard [10] commented that the effects of this technique were not consistent with the infinitesimal limit of the differential.

Rossi [11] noted that by partitioning a blob, when its dimension are too large, in more small blobs (i.e. particle splitting), alleviated the mathematical objection.

Therefore, in conclusion, the CSM consists in alternating core spreading with either core splitting or core merging. Usually, when the spreading makes a blob's core diameter larger than 2 times the initial one, the vortex blob is divided, generally, in four smaller blobs according to conservation criteria of total circulation, linear and angular momentum.

In the following we shall follow the advanced vortex element method, proposed by Kamemoto [12], that sets the boundary condition on the body by considering the velocity field as sum of the asymptotic, of a potential and of a vortical one induced by vortex blobs. The potential field is generated by source panels located on the surface of the body that

take care of setting the normal component of the velocity on the body equal and contrary the local body speed.

The no-slip condition on the body is set up by the introduction of a nascent vortex element within a thin vorticity layer with thickness considered along the body surface $O(1/Re)^{0.5}$.

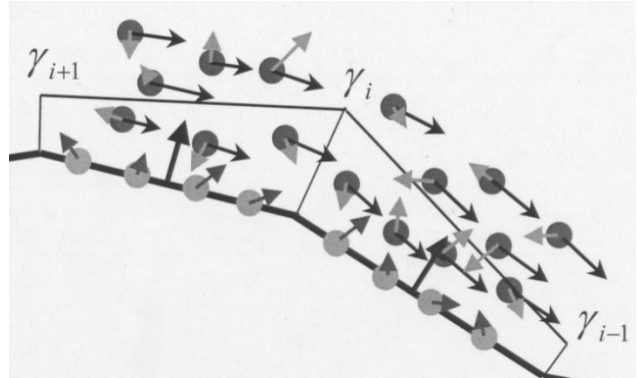


Fig. 4: Nascent vortex sheet to cancel wall slip velocity

The strength of the nascent vortex panel is determined to cancel the slip velocity. When the nascent vortex sheet moves out of the vorticity layer it is replied by an equivalent circular vortex blob of the core spreading model (a Gaussian one).

A 2nd order Adams-Bashfort scheme is used for time integration; pressure in the field and on the body is computed, as post-processing, by integration of an equation formulated by Uhlman [13].

It results a scheme: Simple, Fully local, Embarrassingly parallel.

Advantages of VBM:

- Being Lagrangian methods are typically unsteady;
- Mesh generation is not needed, it is easy to consider complicate geometries;
- Mass conservation is satisfied exactly;
- Robust (CFL condition is removed);
- No numerical dissipation, it is ideal for small scale features;
- They are capable to deal with high value of Reynolds number;
- It is only needed to resolve the rotational part of the flow field and only a small portion of space must be described;

- They are intrinsic adaptive: the motion of the blob secures their presence where needed, so vortex blobs concentrate only in the zones where viscous effects are relevant;
- Rigorous treatment of boundary condition at infinity is implicit.

Disadvantages of VBM:

- Computation of velocity: it is a N-body problem with high computational cost of $O(N^2)$;
- Treatment of diffusive effects (viscosity and heat conduction).

Note that the intrinsic unsteadiness of VBM duly allows to take accounts of the bubble bursting and stall hysteresis, typical features of HLS not always taken into account in early CFD simulations [14].

3. Numerical Experiment

It is fundamental to state that the main scope of this work is not the real full optimization of a HLS at given Reynolds number and angle of attack. In the contest of this paper, we want only to test the use of Vortex Blob Method as a tool for flow visualization in the framework of an optimization process of complicated flow interactions among multi-element airfoils configurations at high Reynolds number of engineering interest.

All the simulations presented were performed with a software package produced by College Master Hands [15] that resulted very handy and productive.

We shall present numerical experiment visualizations to reveal:

1. the separation bubble around clean airfoil;
2. the flow fields for 2-element systems (slat shapes and settings);
3. the flow fields for 3-element systems (slat and flap shapes and settings).

We report Blob paths, vector plots, pressure distributions. Red Blobs particle denotes clockwise (CW) vorticity, cyan Blobs particles denotes counterclockwise (CCW) vorticity.

All the simulations were performed at a $Rey = 0.22 \cdot 10^7$, the same value of the wind tunnel tests available in [16].

3.1 Clean airfoil

We consider the GA(W)-2 airfoil as a base section for development of a HLS. This is a 13% maximum thickness section airfoil derived from the 17% thick GA(W)-1 section. This airfoil was developed in the NASA program for new airfoil sections for the general aviation applications, and has max lift of $C_L=1.7$ at about $\alpha = 15^\circ \div 16^\circ$.

The simulation for $\alpha=18^\circ$ reported in Fig. 5 reveals that two local separations bubbles are present on the top surface of the section, they cause unsteadiness and turbulent reattachment, with definitive flow separation at the rear end.

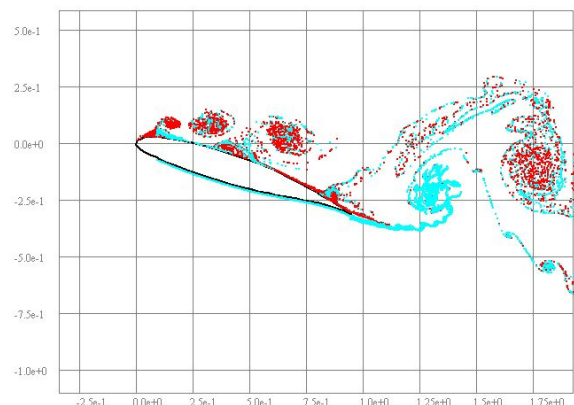


Fig. 5: GA(W)-2 airfoil at $\alpha=18^\circ$, Vortex blob tracks

3.2 Two element configuration: Main and Slat

This HLS system was developed using a 0.14c slat, with shape and setting designed using an instinctive artistic feeling mixed with a technical cut and try process based on the verification of flow field path using the VBM.

Flow details for $\alpha=18^\circ$, on the entire airfoil system (shown by the blob's tracks) are reported in Fig. 6. We note the separated recirculating cave zone, the entrainment of the flow through the slot and the interactions on the top of the main, with confluence of boundary layers and wakes. These interactions generate a quite thick

boundary layer flow, over the main top surface, composed of interlaced vortical layers with different rotation; this causes instability and results in a natural transition toward turbulence. Lower side of the main segment airfoil experiences laminar boundary layer.

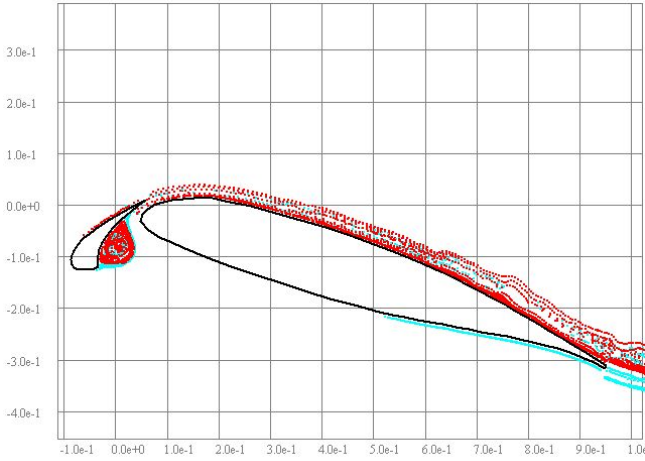


Fig. 6: Main at $\alpha=18^\circ$ with 0.14c Slat, Vortex blob tracks

Fig. 7 reports the details of the leading edge flow, showing the separated recirculated cave zone, the entrainment of the flow through the slot and the interaction on the top of the main, with confluence of boundary layers and wakes.

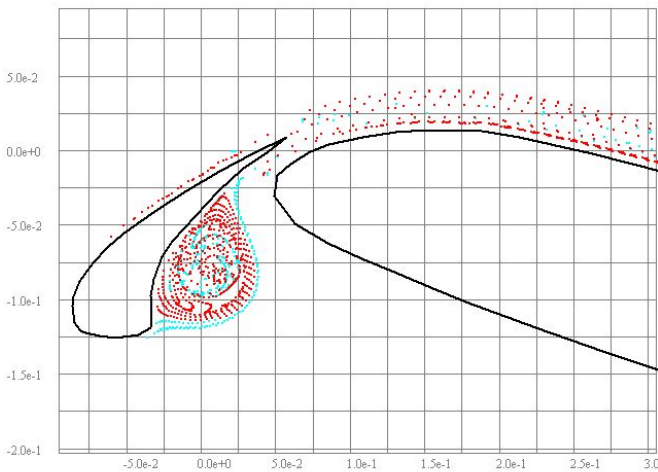


Fig. 7: Main at $\alpha=18^\circ$ with 0.14c Slat, Leading edge detail of Vortex blob tracks.

After many tests, it was argued that the essential point for a good design depends strongly upon the tuning of the slat's angles (depending on α and its geometry) and of its setting (overlap and slot channel gap) relative to

main airfoil segment (all depending on the Reynolds number).

A preliminary requisite for optimum is the achievement of smooth stratification of the fluid wakes and boundary layers over the top surface of the main and to realize a strong mixing process. Note that the alternations of CW and CCW vortical layers, over the main top surface, cause a larger boundary layer thickness (separation problem) with curvature changes in the velocity profiles (instability seed).

Fig. 8 reports the pressure distribution over the said HLS system. The behaviour is as expected, and reveals the favorable A.M.O. Smith's effects. The maximum pressure peak is found to be located on the front top part of the main, and the pressure pick on the slat top surface moves backward toward the slat channel exit. This effect reduces pressure gradient and delays transition and bubbles. The lower surface is characterized by the large recirculation eddy formed in the slat cave that, for good design, is only slightly puffing.

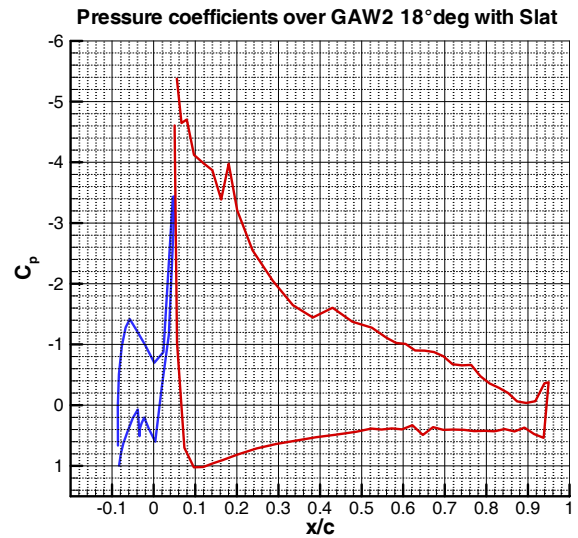


Fig. 8: Main at $\alpha=18^\circ$ with 0.14c Slat, pressure coefficient distribution

As result, some Tollmien-Schicthing like waves travel on both sides of the main. These waves can be recognized by the ripples that can be detected on the pressure distributions (long waves on the lower surface and shorter on the top surface depending on the different local values of the velocity). Trailing edge patterns

depend on the peculiar finite thickness and flow angle of the GA(W)-2 section.

3.3 Three elements configuration: Main, Slat, and Flap

This HLS configuration is derived by the previous one by inserting a 0.39c Fowler flap.

The flap is very similar to the one of [16], but the main's hollow shape is refined by a cut and try process. As before, Fig. 9 depicts the blob track up to $t=1$ sec. At this time the flow on the flap top surface is not yet set since a starting eddy is still present on the flap's top.

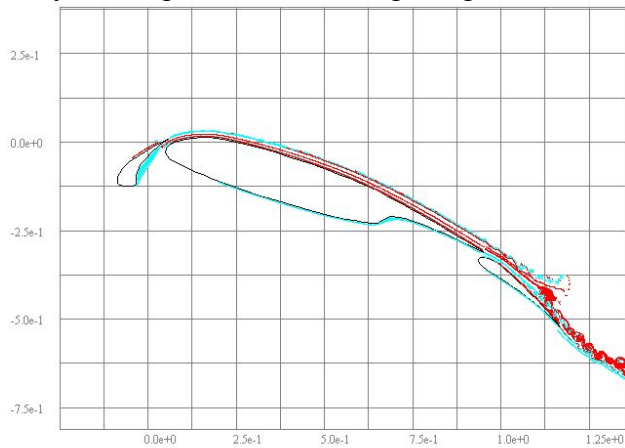


Fig. 9: Main at $\alpha=18^\circ$ with 0.14c Slat and 0.30c Flap

By comparing the vortical boundary layer on main's top of Fig. 9 with Fig. 6 one can understand the A.M.O. Smith's favorable effect of the flap that induces an off-surface pressure recovery on the main by reducing boundary layer thickness and by causing a benefic mixing effect: CW vorticity sheet moves outside stabilizing the whole layer.

Fig. 10 details the flows around the trailing edge at time $t=1.5$ sec. At this stage the initial vortical eddy has moved away from the airfoil and a 5 layers ensemble is established on the flap's top surface. Three layers are coming from the main's top side, one (CW) is relative to boundary layer initiating on the top side of the flap and one (CCW) is from the main's lower side. This latter layer introduces instability and causes natural transition, as visualized by the small turbulent eddies that can be noted on the upper side and from the clearly turbulent wake.

Probably, a slight different setting could set better flow conditions but, as said, this is out the scope of this paper.

Obviously the dynamic of the whole process is better understood and appreciated by looking at the global movies, which the figures are extracted from.

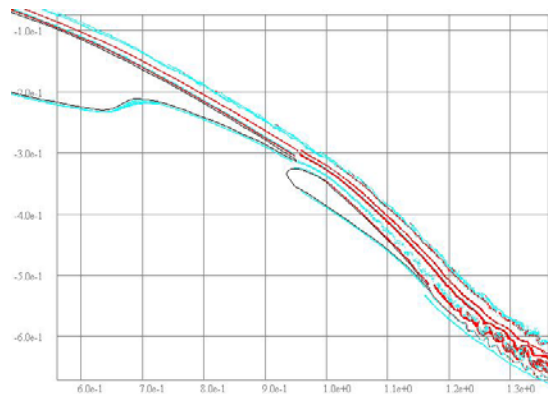


Fig. 10: Main at $\alpha=18^\circ$ with 0.14c Slat and 0.30c Flap, details of trailing edge at $t=1.5$ sec.

Fig. 11 reports the velocity vector plots around the same configuration. The vector colors are set according to the values of the speeds. Details of the velocity field can be better appreciated by enlarging single zones. This enforces the use of the method to generate, with very little work, a CFD unsteady PIV.

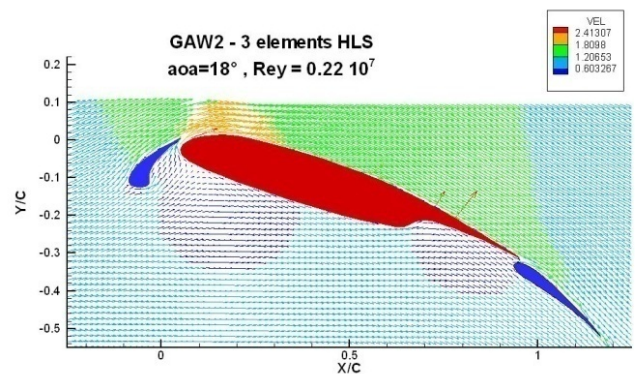


Fig. 11: Main at $\alpha=18^\circ$ with 0.14c Slat and 0.30c Flap, velocity vector

Fig. 12 reports the surface pressure coefficient distributions around the three elements high lift systems. The comments are very similar to the ones relative to Fig. 8. A comparison of the two figures reveals the effects of the flap that causes a pressure recovery on both sides of the main: ripples on the top side of

the main are reduced, pressure levels are large to cause a beneficial increase of the lift load.

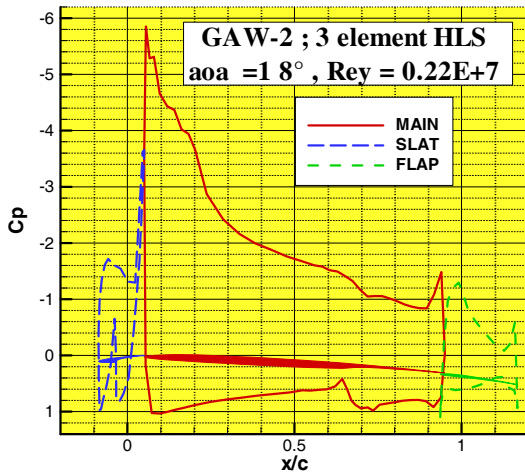


Fig. 12: Main at $\alpha=18^\circ$ with 0.14c Slat and 0.30c Flap, surface pressure distribution

3.4 Comparison of the overall results

Fig. 13 reports the lift coefficient results of the numerical experiments compared with the experimental results for the plain lean section airfoil [16]. We can note that the leading edge and trailing edge devices introduce effects on the lift curve according to the trends described in Fig.1.

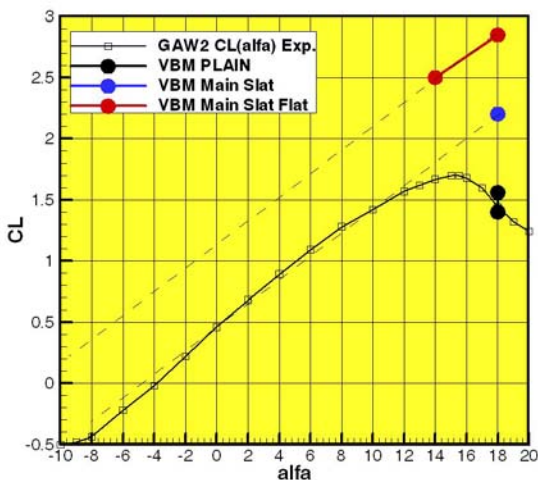


Fig. 13: GA(W)-2 lift curve: experiments and numerical experiment results

Some comments need to be cleared.

Any fluiddynamicist is well aware that in case of large separation zones or recirculating

eddies and in case of turbulent flow and separation the effects on unsteadiness can be relevant. VBM is a real unsteady method that does not introduce any damping and filtering on field variables. Not so with experimental force measurements that are biased by balances inertia and structural damping. VBM steady state conditions are determined as limiting transient evolutions; they cannot be achieved if some unsteadiness is present due to fluid-dynamics physics. A filtering process is the necessary, but if the fluctuation level is quite elevated (such as in case of full stalled conditions) the filtering value is questionable.

In the cases compared in Fig. 13 unsteadiness were low and a comparison is possible; the numerical simulations for the lift coefficient resulted to be reasonable agreeable within $\pm 5\%$. For drag and moment the results are over-estimated, and up to one order of magnitude in case of the moment.

A complete analysis of the accuracies and of the fine details of the cove and jet merging flows is out of the scope of this paper and will be considered in future communications.

4. Conclusions

This paper considers a Lagrangian analysis of two dimensional flow problems described by velocity vorticity formulation. A Vortex Blob Method (VBM) based on Biot-Savart equation is used combined with a BEM for computing the potential velocity field, and with a Core Spreading Method (CSM) for computing the vortex blob diffusion. It results a very simple and efficient instrument to visualize unsteady vortex flow paths within multi-element airfoil components and gaps.

Main scope of the paper is to verify if VBM is apt to describe the physic of the fluid process that occurs in a multi element high lift airfoil system. The main aerodynamic problem lays in the capacity to describe and to recognize the physics of:

- Separation bubbles;
- Re-attachment;
- Re-laminarization;
- Confluence of boundary layer with wakes;

- Steady, intermittent and fully unsteady separated boundary layer.

All these problems are strongly dependent on the values of the flight Reynolds number.

The code is tested by considering plain GA(W)-2 airfoil, and 2 element (slat and main) and 3 element (slat, main, slotted flap) systems there from derived. All these configurations are tested with small variations of the geometries and settings in order to verify the ensuing flow fields and resulting global forces.

Overall and detailed vortical zone flows are visualized by blob tracking. Global velocity plot are easily generated, the same for the surface pressure distributions. The software package code used [15] reveals to function as a handily CFD-PIV machine.

The many testings confirm the capacity of VBM to recognize flow details coherent with geometrical settings. No problem with the simulation of high value of Reynolds number that was set to the same value used in the Wind Tunnel. In case of separated flows the force coefficients suffer of unsteady fluctuations that require adequate filtering for comparison with experimental data.

In general, lift forces are quite accurate, whereas drag and moment are over-estimated

We remark again that no full optimization of a high lifting system has been envisaged, the main scope being to verify if the Vortex Blob Method can be used in the preliminary analysis of high-lift systems. The tests cases were devised to prove if the methods is apt to sense separation, reattachments, transition physics, and if the effects on flow produced by settings variation are as expected.

In conclusion, VBM is a very simple and productive tool and, at the present status, can be of help in the preliminary phase of design and optimization phase, but a final check with traditional CFD is needed for accurate forces evaluation.

Acknowledgements

The author express the deepest senses of gratitude to prof. Kamemoto for having stimulated the interest in vortex method, and to College Master Hands, inc. for the cooperation in the package codes.

References

- [1] C.P. van Dam. The aerodynamic design of multi-element high-lift systems for transport airplanes, *Progress in Aerospace Sciences* 38, 101–144, 2002.
- [2] Rudolph PKC. High-lift systems on commercial subsonic airliners, *NASA CR 4746*, 1996.
- [3] Meredith P. Viscous phenomena affecting high-lift systems and suggestions for future CFD development, in High-Lift System Aerodynamics, *AGARD CP 515*, pp. 19-1–19-8, 1993.
- [4] Smith A.M.O. High-lift Aerodynamics, *Journal of Aircraft* 12(6), 501–530, 1975.
- [5] Rumsey C.L., Ying S.X. Prediction of high lift: review of present CFD capability, *Progress in Aerospace Sciences* 38, 145-180, 2002.
- [6] Stock, M.J., Summary of Vortex method Literature, available from: <http://mark.technolope.org/research/> [Accessed 9 November 2007].
- [7] Chorin, A.J. Numerical Study of Slightly Viscous Flow, *J. Fluid Mechanics* 57 (4), 785-796, 1973.
- [8] Kuwara, K., Takami, H.. Numerical Studies of Two-Dimensional Vortex Motion by a System of Point Vortices, *Journal of the Physical Society of Japan* 34 (1), 247-253, 1973.
- [9] Leonard, A Vortex Methods, *Journal of Computational Physics* 37, 289-335, 1980.
- [10] Greengard, L. The core spreading v.m. approximate the wrong equation, *Journal of Computational Physics* 61, 345-348, 1985.
- [11] Rossi, L.F. Resurrecting Core Spreading Methods, *SIAM J. Sci. Comp.* 17 (2), 370-397, 1996.
- [12] Kamemoto, K. On Contribution of Advanced Vortex Element Methods Toward Virtual Reality of Unsteady Vortical Flows in the New Generation of CFD - *J. of the Braz. Soc. of Mech. Sci. & Eng.* 26 (4), 368-378, 2004.
- [13] Uhlman, J.S. An integral formulation of the equation of motion of an incompressible fluid, *Naval Undersea Warfare Center T.R.* 10-086, 1992.
- [14] Baragona M., Boermans L.M.M., van Tooren M.J.L., Bijl H., Beukers A. Bubble bursting and stall hysteresis on single-slotted flap high-lift configuration, *AIAA Journal* 42 (7), 1230-1237, 2003.
- [15] College Master Hands, inc. URL <http://www.cmhands.com>
- [16] Wentz, W.H. Jr. Wind Tunnel Test of the GA(W)-2 airfoil... , *NASA CR-145139*, 1997.

Copyright Statement

The authors confirm that they, and/or their company or institution, hold copyright on all of the original material included in their paper. They also confirm they have obtained permission, from the copyright holder of any third party material included in their paper, to publish it as part of their paper. The authors grant full permission for the publication and distribution of their paper as part of the ICAS2008 proceedings or as individual off-prints from the proceedings.